An Analytical Model for Injectivity Tests in Multilayered Reservoir with Formation Crossflow

Isabela Vasconcellos Viana; Renan Vieira Bela; Sinesio Pesco; Abelardo Barreto Junior

PUC-Rio

Corresponding Author: Isabela V. Viana
E-mail: isabelaviana@aluno.puc-rio.br

Abstract

The injectivity tests consist of injecting a phase, usually water, through wells into an oil reservoir in order to collect information about its parameters. Knowing these reservoir's parameters can be valuable in order to improve oil production. In that sense, many studies concerning injectivity tests in multilayered reservoirs have been presented. However, these studies regard only commingled systems, that is, layers that are separated by impermeable barriers. Therefore, the present work developed an analytical model in the Laplace space for multilayered reservoirs under injectivity tests considering formation crossflow along all its layers. The accuracy of the proposed solution was verified by comparison with a finite difference flow simulator. The results provided by the analytical model and by the numerical data were consistently similar. Furthermore, the data obtained by the analytical solution was used to estimate the reservoir's equivalent permeability. Calculated values presented a satisfactory accuracy for all cases.

1. Introduction

An injectivity test consists on injecting water into an oil reservoir and, in response to that, many significant information about the reservoir can be inferred, which can be valuable in order to improve the oil production. For instance, equivalent permeability, outer boundary condition and recoverable oil volume can be inferred. The way of detecting those pieces of information is through analyzing the pressure transient response. In this work, an analytical solution is proposed concerning multilayered reservoirs with formation crossflow.

Formation crossflow, different than wellbore crossflow, happens when there is a nonzero vertical permeability at the interface between two adjacent layers. In this work formation crossflow was defined like in the work of Sun and Gao (2017), which presented a semipermeable-wall system. Besides formation crossflow, this work will consider that all layers properties, such as porosity, permeability and thickness, may be different in each layer.

Based on Sun and Gao (2017), the work proposed by Ehlig-Economides and Joseph (1987), presented an analytical model for a multilayered reservoir under single phase flow considering formation crossflow. Properties may also be different from layer to layer. In addition, the work presented by Ehlig-Economides and Joseph (1987), was developed in the Laplace field and used numerical inversion of Laplace transforms, more specifically, the Stehfest Algorithm (Stehfest, 1970) in order to find a pressure response in the real field. The present work will also be presented in the Laplace field and the Stehfest algorithm will be used in order to convert it into the real field.

The formulation proposed in this work, combines the formation crossflow feature with a two phase flow model. To model the two phase flow composition, this work was based on the one presented by LF Bittencourt Neto et al. (2020b) which extended the solution from a model for a radially composed reservoir under single phase flow as in given by LF Bittencourt Neto et al. (2020a), because during injectivity tests in a homogeneous reservoir, there are still different regions, but in respect to the fluids. The formulation proposed by LF Bittencourt Neto et al. (2020a) was also done in the Laplace domain, considered different properties in a two-layered model. Furthermore, in LF Bittencourt Neto et al. (2020b), a single layered reservoir was considered and formation crossflow was unconsidered.

The work proposed by Barreto et al. (2011), presented a model for injectivity tests like in the work of Bratvold et al. (1990), however Barreto et al. (2011) considered a multilayered reservoir. The solution proposed by Barreto et al. (2011) for the injection period assumes, like the present work, a radially infinite reservoir. Both the works proposed by Bratvold et al. (1990) and Barreto et al. (2011) did not considered formation crossflow.

This present work is innovating as it presents a formulation considering formation crossflow for multilayered reservoirs under injectivity tests. This paper will be divided, essentially, in description of the model, mathematical formulation, results and discussions and conclusions.

2. Model Description

Before the injectivity test begins, the reservoir is filled with single phase solution (oil), then, the injection of water in the oil reservoir begins, establishing the two phase fluid flow scenario. For this case, consider an infinite, multilayered, homogeneous and isotropic reservoir. In addition, it has an oil viscosity (μ_o) that is constant, as well as constant water viscosity (μ_w). It also has constant and small total compressibility (c_t).The porosity (ϕ_j) may have a different value in each layer, as well as the thickness (h_j). Constant flow rate is considered. Formation damage and wellbore storage will be disregarded. Moreover, consider a piston-like displacement, i.e., the water front in each layer advances uniformly. All the formulation was done in consistent units.

Even though the rock properties within each layer are the same, there are different composition properties within them, such as viscosity. Hence, this two phase flow model can be represented by a two regions model with moving boundary, with the water region increasing with time. Because of their similarities, the single phase model for composite reservoirs can be extended to model the two phase case LF Bittencourt Neto et al. (2020b).

Constant layer flow rates and thicknesses will be considered and there is formation crossflow within these layers. In each layer, region 1 will represent the region that contains the water being injected and region 2 the region that contains oil only. Figure 1 represents that system:

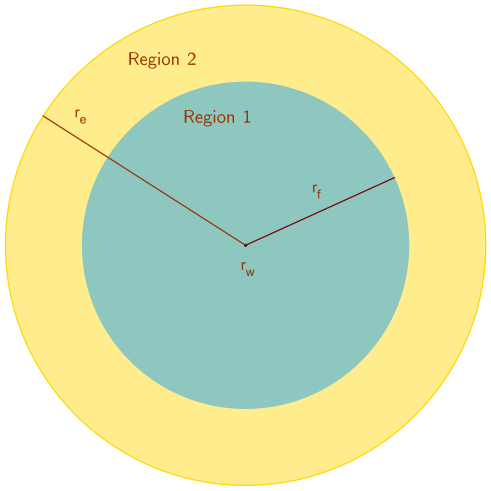

Fig. 1 – Two phase fluid flow in a reservoir

In figure 1, r_w is the radius of the injector well, r_f the water front radius, which will be defined later for each time t and r_e is the external radius. Consider $\Delta p_{ji} = p_{ji} - p_i$, the pressure change in each layer $j = 1, 2, \ldots, n$ is governed by the following diffusion equation for each region of fluid $i = w, o$:

$$(kh)_j \nabla^2 \Delta p_{ji} = (\phi h)_j c_t \mu_i \frac{\partial \Delta p_{ji}}{\partial t} + (\Delta p_{ji} - \Delta p_{(j-1)F}) X_{j-1} - (\Delta p_{(j+1)F} - \Delta p_{ji}) X_j \quad [1]$$

The coefficient of semipermeability X_j is given as in Ehlig-Economides and Joseph (1987) for layers j and $j+1$ relating the permeabilities of each one of this layers:

$$X_j = \frac{2}{2[(\Delta h_j)/k_{vj}] + \chi_{j+1} + \chi_j} \quad [2]$$

where $X_n = X_0 = 0$. Δh_j and k_{v_j} are the thickness and the permeability of shale between layers j and $j+1$ and χ_j is defined as:

$$\chi_j = \frac{h_j}{k_{z_j}} \quad [3]$$

where k_{z_j} is the vertical permeability of layer j. If there is no formation crossflow between layers j and $j+1$ then, X_j is zero.

Observing the reservoir laterally, figure 2 illustrates this model for a two layered case:

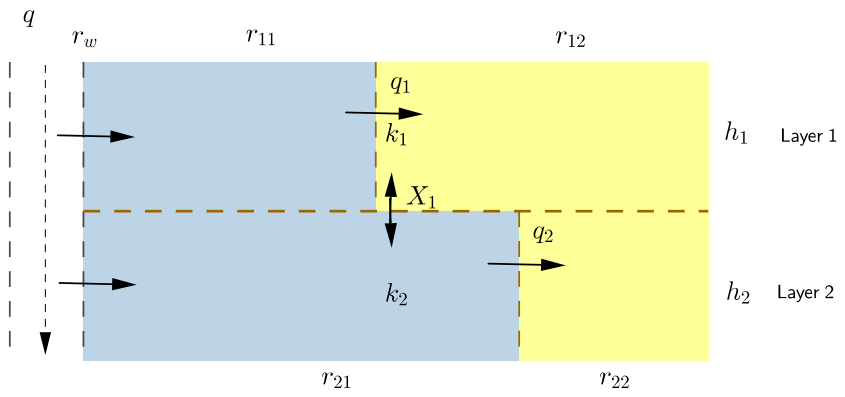

Fig. 2 – Two phase fluid flow in a two layer reservoir with formation crossflow

Notice that, since a single region of permeability is considered per layer, there is only a single semipermeability coefficient in each adjacency. Eq.(2) evidences that only the rock properties are considered which are the same for all layers. If there were more regions in respect to the permeability, there would be more semipermeability coefficients.

Now, consider the volume injected in layer j (Barreto et al., 2011):

$$v_j(t) = \int_0^t q_j(t')dt' \quad [4]$$

To calculate the water front radius (r_F) for each layer j the formula given by Buckley et al. (1942) for cylindrical geometry is considered:

$$r_{jF}(t) = \sqrt{(r_w)^2 + \frac{v_j B_w}{24\pi\phi_j h_j} f'_{wj} t} \quad [5]$$

where f'_{wj} represents the derivative of the curve of fractional flow of water at layer j at each point of fluid saturation. Since a piston flow is considered, f'_{wj} is given by (LF Bittencourt Neto et al., 2020b):

$$f'_{wj} = \frac{1}{1 - S^j_{or} - S^j_{wi}} \quad [6]$$

Here S^j_{or} is the oil residual saturation and S^j_{wi} is the irreducible water saturation in layer j. The water and oil fluid mobility of layer j ($\hat{\lambda}^j_i$), which will be used in the initial boundary condition, are defined as:

$$\hat{\lambda}^j_i = \frac{k^{ri}_j k_j}{\mu_i}, \text{ where } i = w, o \quad [7]$$

Here k^{ri}_j is the permeability of layer j related to phase in region i and k_j is layer j permeability.

3. Mathematical Formulation

The formulation presented in this section was mainly extended from the work by Ehlig-Economides and Joseph (1987) for the formation crossflow consideration and from the work by LF Bittencourt Neto et al. (2020a) for the extension of a radial composite reservoir for a two phase formulation.

Considering the hypotheses from the previous section, the model description is given by the diffusion equation [1] and its suitable boundary conditions:

- The Initial Condition (I.C.) which occurs at time $t = 0$ and reflects that the reservoir is initially in balance, that is, the pressure is the same in all layers (apart from the hydrostatic effect).
- The Internal Boundary Condition (I.B.C) which is related to the fluid injection in each layer.
- The External Boundary Condition (E.B.C) which refers to the flow behavior at the extreme limit of the reservoir and, in this work, an infinite-like reservoir is considered.

Consider $\kappa_j = (k_j h_j)$ and $\omega_j = (\phi_j h_j)$ and let i index each region of phase $F = w, o$, then the following equations model the problems for all layers $j = 1, \ldots, n$ and regions $i = 1, 2$ (Lefkovits et al., 1961; Ehlig-Economides and Joseph, 1987):

Region 1 ($r_w < r < r_{jF}$):

$$PDE : \kappa_j \nabla^2 \Delta p_{j1} = \omega_j c_t \mu_w \frac{\partial \Delta p_{j1}(r,t)}{\partial t} + (\Delta p_{j1} - \Delta p_{(j-1)1}) X_{j-1} - (\Delta p_{(j+1)1} - \Delta p_{j1}) X_j;, \; t > 0 \quad [8]$$

$$IC : \quad \Delta p_{j1}(r, 0) = 0 \quad [9]$$

$$IBC : \quad q_{j1} = -2\pi \hat{\lambda}_w h \Big(r \frac{\partial \Delta p_{j1}}{\partial r} \Big) \Big|_{r=r_w} \quad [10]$$

Region 2 ($r > r_{jF}$):

$$PDE : \kappa_j \nabla^2 \Delta p_{j2} = \omega_j c_t \mu_o \frac{\partial \Delta p_{j2}(r,t)}{\partial t} + (\Delta p_{j2} - \Delta p_{(j-1)2}) X_{j-1} - (\Delta p_{(j+1)2} - \Delta p_{j2}) X_j;, \; t > 0 \quad [11]$$

$$IC : \quad \Delta p_{j2}(r, 0) = 0 \quad [12]$$

$$EBC : \lim_{r \to \infty} \Delta p_{j2}(r = \infty, t) = 0 \quad [13]$$

When $j = 1$, $X_{j-1} = 0$ and when $j = n$, $X_j = 0$. Consider $\overline{p}_{ji}$ to be the Laplace transform of the pressure variation and u to be the Laplace's variable, then, in the Laplace field, equations [8] to [13] become:

Region 1:

$$ODE : \kappa_j \nabla^2 \Delta \overline{p}_{j1} = \omega_j c_t u \mu_w \Delta \overline{p}_{j1} + (\Delta \overline{p}_{j1} - \Delta \overline{p}_{(j-1)1}) X_{j-1} - (\Delta \overline{p}_{(j+1)1} - \Delta \overline{p}_{j1}) X_j; \; r_w < r < r_{jF} \quad [14]$$

$$IBC : \quad \overline{q}_{j1} = -2\pi \hat{\lambda}_w h \Big(r \frac{\partial \Delta \overline{p}_{j1}}{\partial r} \Big) \Big|_{r=r_w} \quad [15]$$

Region 2:

$$ODE : \kappa_j \nabla^2 \Delta \overline{p}_{j2} = \omega_j c_t u \mu_o \Delta \overline{p}_{j2}(r,t) + (\Delta \overline{p}_{j2} - \Delta \overline{p}_{(j-1)2}) X_{j-1} - (\Delta \overline{p}_{(j+1)2} - \Delta \overline{p}_{j2}) X_j; \; r > r_{jF} \quad [16]$$

$$EBC : \lim_{r \to \infty} \Delta \overline{p}_{12}(r = \infty, t) = 0 \quad [17]$$

The coupling conditions between regions 1 and 2 (CCR) are given by the flow rate and pressure equalities at the water front radius in each layer j (LF Bittencourt Neto et al., 2020a; Nie et al., 2011):

$$CCR = \begin{cases} \Delta \overline{p}_{11}(r = r_{1F}, t) = \Delta \overline{p}_{12}(r = r_{1F}, t) \\ \Delta \overline{p}_{21}(r = r_{2F}, t) = \Delta \overline{p}_{22}(r = r_{2F}, t) \\ \vdots \\ \Delta \overline{p}_{n1}(r = r_{nF}, t) = \Delta \overline{p}_{n2}(r = r_{nF}, t) \\ \overline{q}_{11} = \overline{q}_{12} \\ \overline{q}_{21} = \overline{q}_{22} \\ \vdots \\ \overline{q}_{n1} = \overline{q}_{n2} \end{cases} \quad [18]$$

Using Darcy's law, the flow rate CCRs can be replaced:

$$CCR = \begin{cases} \Delta\overline{p}_{11}(r = r_{1F}, t) = \Delta\overline{p}_{12}(r = r_{1F}, t) \\ \Delta\overline{p}_{21}(r = r_{2F}, t) = \Delta\overline{p}_{22}(r = r_{2F}, t) \\ \vdots \\ \Delta\overline{p}_{n1}(r = r_{nF}, t) = \Delta\overline{p}_{n2}(r = r_{nF}, t) \\ \left(r\frac{\partial\Delta\overline{p}_{11}}{\partial r}\right)\Big|_{r=r_{1F}} = \frac{\hat{\lambda}_o}{\hat{\lambda}_w}\left(r\frac{\partial\Delta\overline{p}_{12}}{\partial r}\right)\Big|_{r=r_{1F}} \\ \left(r\frac{\partial\Delta\overline{p}_{21}}{\partial r}\right)\Big|_{r=r_{2F}} = \frac{\hat{\lambda}_o}{\hat{\lambda}_w}\left(r\frac{\partial\Delta\overline{p}_{22}}{\partial r}\right)\Big|_{r=r_{2F}} \\ \vdots \\ \left(r\frac{\partial\Delta\overline{p}_{n1}}{\partial r}\right)\Big|_{r=r_{nF}} = \frac{\hat{\lambda}_o}{\hat{\lambda}_w}\left(r\frac{\partial\Delta\overline{p}_{n2}}{\partial r}\right)\Big|_{r=r_{nF}} \end{cases} \quad [19]$$

Between layers, there is also a coupling condition, the CCL. This condition is obtained considering that the pressure change in both layers is equal at the well and that the flow rate at the well is given by the sum of the flow rates of each layer (LF Bittencourt Neto et al., 2020a):

$$CCL = \begin{cases} -\frac{q}{u} = \sum_{j=1}^{n} \overline{q}_{j1} \\ \Delta\overline{p}_{11}(r = r_w, t) = \Delta\overline{p}_{21}(r = r_w, t) \\ \Delta\overline{p}_{21}(r = r_w, t) = \Delta\overline{p}_{31}(r = r_w, t) \\ \vdots \\ \Delta\overline{p}_{(n-1)1}(r = r_w, t) = \Delta\overline{p}_{n1}(r = r_w, t) \end{cases} \quad [20]$$

Once again, the flow rate equation can be rewritten using Darcy's law:

$$CCL = \begin{cases} -\frac{q}{2\pi u r_w(\hat{\lambda}_w^1 h_1 + \hat{\lambda}_w^2 h_2 + \ldots + \hat{\lambda}_w^n h_n)} = \sum_{j=1}^{n} \frac{\partial\Delta\overline{p}_{j1}}{\partial r}\Big|_{r=r_w} \\ \Delta\overline{p}_{11}(r = r_w, t) = \Delta\overline{p}_{21}(r = r_w, t) \\ \Delta\overline{p}_{21}(r = r_w, t) = \Delta\overline{p}_{31}(r = r_w, t) \\ \vdots \\ \Delta\overline{p}_{(n-1)1}(r = r_w, t) = \Delta\overline{p}_{n1}(r = r_w, t) \end{cases} \quad [21]$$

There is a general pressure solution for equations [14] and [16] given in terms of the Bessel modified functions (Ehlig-Economides and Joseph, 1987):

Region 1 (water):

$$\Delta\overline{p}_{j1} = A_j^1 K_0(r\sigma_{j1}) + B_j^1 I_0(r\sigma_{j1}) \quad [22]$$

Region 2 (oil):

$$\Delta\overline{p}_{j2} = A_j^2 K_0(r\sigma_{j2}) + B_j^2 I_0(r\sigma_{j2}) \tag{23}$$

For $j = 1, \ldots, n$.

Applying the EBC in the general solution given for region 2:

$$\lim_{r\to\infty}\left[A_j^2 K_0(\sigma_{j2}r) + B_j^2 I_0(\sigma_{j2}r)\right] = 0 \tag{24}$$

Knowing the properties for Bessel's modified functions, it is true that:

$$\lim_{r\to\infty}\left[B_j^2 I_0(\sigma_{j2}r)\right] = 0 \iff B_j^2 = 0 \tag{25}$$

Hence, the pressure solution for region 2 is given by:

$$\Delta\overline{p}_{j2} = A_j^2 K_0(\sigma_{j2}r) \tag{26}$$

Calculating the laplacian of both solutions:

$$\nabla^2\Delta\overline{p}_{j1} = \sigma_{j1}^2(A_j^1 K_0(r\sigma_{j1}) + B_j^1 I_0(r\sigma_{j1})) = \sigma_{j1}\Delta\overline{p}_{j1} \tag{27}$$

$$\nabla^2\Delta\overline{p}_{j2} = \sigma_{j2}^2(A_j^2 K_0(r\sigma_{j2})) = \sigma_{j2}\Delta\overline{p}_{j2} \tag{28}$$

Replacing the equivalences above into the ODEs [14] and [16]:

$$(\kappa_j\sigma_{ji}^2 - \omega_j c_t \mu_{ji} u - X_{j-1} - X_j)\Delta\overline{p}_{ji} + X_{j-1}\Delta\overline{p}_{(j-1)i} - X_j\Delta\overline{p}_{(j+1)i} = 0 \tag{29}$$

This is a homogeneous linear system for each region i where the nontrivial solution is wanted, that is, $\Delta\overline{p}_{ji} \neq 0$. That is true only if each matrix below is singular, and that implies that its determinant must vanish:

$$a^i_{jk} = \begin{cases} X^i_{j-1}, & \text{for } k = j-1; j > 1, \\ \kappa_{ji}\sigma^2_{ji} - \omega_j c_t \mu u - X^i_{j-1} - X^i_j, & \text{for } k = j, \\ X^i_j, & \text{for } k = j+1; j < n, \\ 0, & \text{for } k \neq j-1, j, \text{or } j+1. \end{cases} \quad [30]$$

For $i = 1, 2$.

Now, with the values of σ_{ji} calculated by letting $det(a^i_{jk}) = 0$, the coefficients of the pressure solution must be found in order to calculate the pressure variation. The coupling conditions are used for that end. Replacing equations [22] and [26] in each CCR and CCL the following equations are obtained:

Pressure CCL:

$$A^1_{j-1}K_0(\sigma_{(j-1)1}r_w) + B^1_{j-1}I_0(\sigma_{(j-1)1}r_w) = A^1_j K_0(\sigma_{j1}r_w) + B^1_j I_0(\sigma_{j1}r_w) \quad [31]$$

For $j = 2, ..., n$.

Flow rate CCL:

$$\sigma_{11}(A^1_1 K_1(r_w\sigma_{11}) - B^1_1 I_1(r_w\sigma_{11})) + \ldots + \sigma_{n1}(A^1_n K_1(r_w\sigma_{n1}) - B^1_n I_1(r_w\sigma_{n1})) = \frac{q}{2\pi u r_w \sum_{j=1}^{n} \hat{\lambda}^j_w h_j} \quad [32]$$

Pressure CCR:

$$A^1_j K_0(\sigma_{j1}r_{j1}) + B^1_j I_0(\sigma_{j1}r_{j1}) = A^2_j K_0(\sigma_{j2}r_{j1}) \quad [33]$$

For $j = 1, ..., n$.

Flow rate CCR:

$$A^1_j K_1(r_{jF}\sigma_{jw}) - B^1_j I_1(r_{jF}\sigma_{jw}) = \frac{\hat{\lambda}_o}{\hat{\lambda}_w}\frac{\sigma_{jo}}{\sigma_{jw}}[A^2_j K_1(r_{jF}\sigma_{jo})] \quad [34]$$

For $j = 1, ..., n$.

Relations [31], [32], [33] and [34] provide a $3n$ equations that form a linear system to calculate the pressure coefficients A^1_j, B^1_j and A^2_j:

$$\begin{bmatrix} A^1_1 \\ B^1_1 \\ A^2_1 \\ A^1_2 \\ B^1_2 \\ A^2_2 \\ \vdots \\ A^1_n \\ B^1_n \\ A^2_n \end{bmatrix} = M^{-1} \begin{bmatrix} \frac{q}{2\pi u r_w \sum_{j=1}^{n} \hat{\lambda}^j_w h_j} \\ 0 \\ 0 \\ 0 \\ 0 \\ 0 \\ \vdots \\ 0 \\ 0 \\ 0 \end{bmatrix}$$

where M is formed using equations [31] to [34], and finally, it is possible to calculate the pressure variation at the wellbore:

$$\Delta\overline{p}_{wf} = A_1^1 K_0(\sigma_{11} r_w) + B_1^1 I_0(\sigma_{11} r_w) \quad [35]$$

Pressure profile is given by equation [35] in the Laplace field. Using the Stehfest (1970) Algorithm, this solution is given in the real field.

4. Results and Discussions

The results for the wellbore pressure profile for the analytical model proposed is presented in this section. A set of cases reflecting the model are presented and the accuracy of the proposed solution was testified by comparing it with a commercial finite difference-based flow simulator CMG (2010). In addition, an estimation of the equivalent permeability was presented and compared it to its real value for all cases.

As an input for the numerical simulation, a radial grid was considered. The grid is more refined in the region closest to the wellbore, which is the region most affected by its presence. The oil model used in the simulator was blackoil. For all cases, formation crossflow is considered between the adjacent layers.

The following parameters were considered:

- 4 days (96 hours) injection period;
- A piston-like flow;
- Injection flow rate was defined as 500 m^3/day (5.79×10^3 m^3/s);
- Initial pressure was defined as 300 kgf/cm^2;
- The wellbore radius was considered to be $r_w = 0.108$ m in all cases;
- Water viscosity will always be considered to be $\mu_w = 0.5$ cP;
- The vertical permeability was considered to be equal to the horizontal permeability for all cases;
- S_{or}^j and S_{wi}^j are considered to be 0 and f'_{wj} is calculated as in eq.(6);
- The thickness of the shale between the layers (Δh) is considered to be zero in all cases for both the analytical and the numerical models.

In order to best evaluate the efficiency of the model, the mobility ratio is considered as a parameter for all cases in each layer, and it is given by (LF Bittencourt Neto et al., 2020b):

$$\hat{M}_j = \frac{\hat{\lambda}_j^w}{\hat{\lambda}_j^o} \quad [36]$$

The mobility ratio, is directly connected to the sweep efficiency of a reservoir. Low mobility ratios ($M < 1$) imply in better sweep efficiency, as oil flows more easily throughout the reservoir. On the other hand, high mobility ratios lead to uneven fronts, reducing the swept reservoir area (LF Bittencourt Neto et al., 2020b).

Other relevant parameters can be found in table 1 for all cases considered:

Case	Properties	Layer 1	Layer 2	Layer 3
A	k(mD)	500	1000	-
	h(m)	15	15	-
	μ_o(cP)	5.1		-
	$\hat{M}$	10.2	10.2	
B	k(mD)	500	600	700
	h(m)	15	15	15
	μ_o(cP)	0.1		
	$\hat{M}$	0.2	0.2	0.2
C	k(mD)	1000	600	300
	h(m)	15	15	15
	μ_o(cP)	3.5		
	$\hat{M}$	7	7	7

Table 1 – Analyzed Cases

In addition, in the graphs of all cases, besides the pressure change curves for the analytical and numerical solutions, the curves of pressure derivatives with respect to the logarithm of time is also present. It is important to analyze the behavior of the pressure derivative as well, in order to properly interpret the results of the test. The curve composed by blue circles denoted the analytical solution for pressure variation and the curve composed by red circles denotes the analytical solution for pressure derivative. For the numerical solutions, yellow stars curve represents the pressure variations and purple stars the derivative curve.

First, case A is analyzed. For this case, a two layer model with different values of permeability in each layer is considered. Pressure and pressure derivative curves for the analytical model solution and numerical solution are presented in figure 3 for case A:

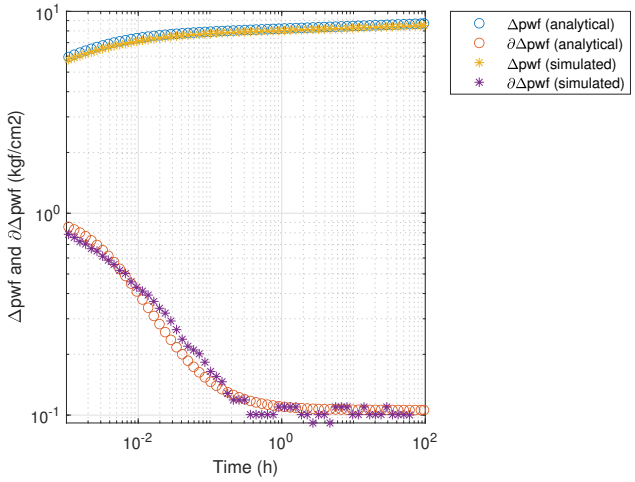

Fig. 3 – Analytical and numerical pressure variation and derivative solutions for case A

Even though there are no different regions of permeability in the layers for this case, the derivative curves behaves as if there were. That is because, the regions of equal permeability are filled with different fluids. The oil and water viscosity values for this case, causes the value of the mobility ratio $\hat{M}$ to be grater than 1, implying on higher pressure derivative values on early times. It is possible to see a close agreement between the analytical and numerical simulated curves.

Case B considers a value of oil viscosity of $\mu_o = 0.1$ cP, which was 5 times smaller than the water's. Implying on a value lower than 1 for $\hat{M}$, in this case it was 0.2. This case also considers different values of permeability per layer. The graphs for pressure and pressure derivative for case B are represented in figure 4:

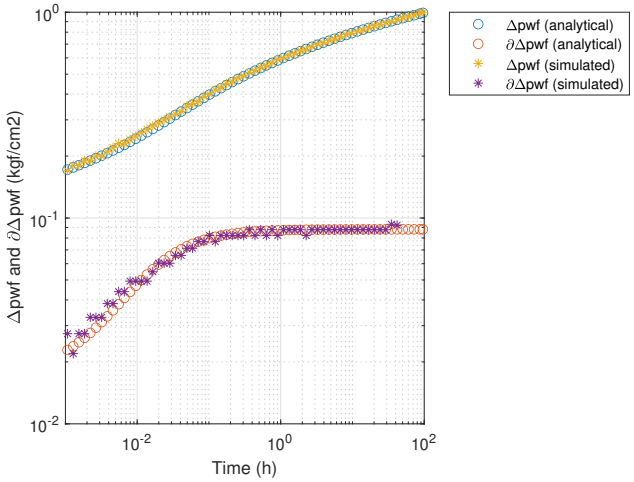

Fig. 4 – Analytical and numerical pressure variation and derivative solutions for case B

It is possible to see that the values in the derivative curves at initial times were five times smaller than in the final times. The derivative curves were increasing because $\hat{M} < 1$ and the sweep efficiency was improved. There was a close agreement between the numerical and analytical curves for this case also.

Finally, case C is considered. That case considers three layers with different properties and $\mu_o = 3.5$ cP. The graphs for pressure and pressure derivative for this case are presented in figure 5:

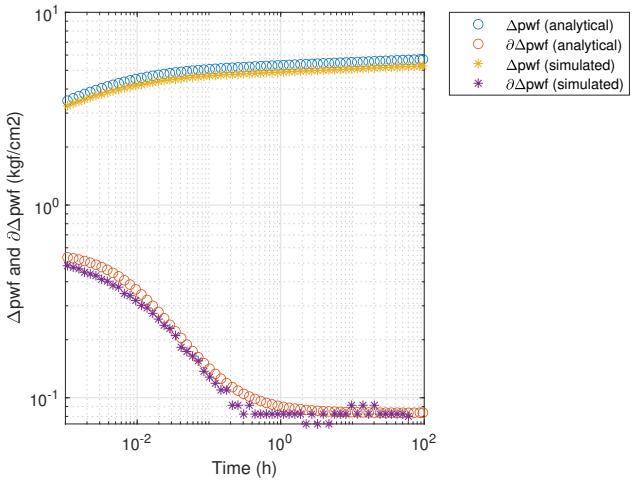

Fig. 5 – Analytical and numerical pressure variation and derivative solutions for case C

Similarly to case A, case C has $\hat{M} > 1$, however, since the difference between the fluids viscosity values is not as big as in case A, the difference in the values of the derivative curves is not as great. There was a small, and apparently constant, difference between the analytical and numerical pressure curves. One reason for that might be because there is a big difference in the permeabilities values from one layer to another causing a bigger awareness of the presence of formation crossflow in the reservoir, and the way the simulator includes the crossflow is different than the way presented in this work. However, the behavior of

the curves is still very similar, resulting in a fair approximation.

A. Equivalent Permeability. The pressure measured at the well is directly linked to the equivalent permeability (k_{eq}). In that sense, another way to evaluating the efficiency of the model presented in this work is by estimating the equivalent permeability.

For a multilayered reservoir, like presented in Cobb et al. (1972), it is given by:

$$k_{\text{eq}} = \frac{\sum_{j=1}^{n} k_j h_j}{\sum_{j=1}^{n} h_j} \tag{37}$$

Since the model presented here reduces the cases of different regions radii into one with regions of equal radii, then the derivative profile enables the computation of equivalent permeabilities that combine the respective regions of the layers. That is, to obtain the first equivalent permeability, region 1 of layer 1 is combined with region 1 of layer 2 and so on.

Using the source line logarithmic approximation, the following equation is used to estimate the equivalent permeability, derived from the single phase formulation(Cobb et al., 1972):

$$\overline{k}_{\text{eq}} = \frac{q\mu_o}{2h_T m} \tag{38}$$

where m is the constant derivative level and h_T is the total thickness.

In table 2, the estimated and real equivalent permeabilities for the region filled with water, are presented for the cases considered in this chapter along with the percentage errors of the approximation:

Case	k_{eq} real (mD)	k_{eq} estimated (mD)	Error (%)
A	750	748.24	0.49
B	600	600.33	0.01
C	633.33	629.64	1.48

Table 2 – Real and estimated equivalent permeability values and percentage error for cases A to C

The cases presented errors less than 2%. This indicates that the proposed formulation may be useful in obtaining reservoir parameters.

5. Conclusions and Suggestions for Future Work

To the best of the authors´ knowledge, this model to solve the injectivity test pressure response problem using a radial composite approach, considering formation crossflow, has never been presented in literature before.

Based on the work presented by Ehlig-Economides and Joseph (1987) which considered formation crossflow, the present work extended it for a two phase model using a composed reservoir approach.

For all cases, a close agreement between the approximated analytical solution and numerical data was achieved. Results show that the suggested analytical model is able to describe pressure behavior in multilayered reservoirs during injectivity tests using a radial composite approach. Furthermore, results show a small error when comparing the estimated equivalent permeability to the real ones for all cases

presented. This work extends the comprehension of pressure behavior to a wider range of scenarios and the results obtained might be used to reservoir management applications.

The presented solution considers a zero skin factor. A solution which considers different values of the skin factor is of practical interest. In addition, this work considers a single region of permeability in each layer. A solution which considers multiple regions of permeability per layer is also of practical interest. For the implementation of that last suggestion, there would be more semipermeability coefficients per adjacency.

6. Nomenclature

a_{jk} - Matrix elements
A_j^i, B_j^i - Coefficients for jth layer and ith region defined in the pressure solution
c_t - Total system compressibility
h_j - Thickness of layer j
h_T - Total reservoir thickness
I_i, K_i - Modified Bessel functions of first and second kind and order i
k_{eq} - Reservoir equivalent permeability
k_j^i - Horizontal permeability in layer j and region i
n - Number of layers in reservoir system
m_j - Number of regions in layer j
p_i - Initial Pressure
p_j^i - Reservoir pressure in layer j and region i
Δp - Pressure change $\overline{p}$ - Pressure change in the Laplace domain
p_{wf} - Well-bottom hole pressure
q_{ji} - Flow rate for layer j and region i
r - Radius
r_j^i - Radius of region i in layer j
r_e - Reservoir outer radius
r_w - Wellbore radius
t - Time
u - Laplace variable
X_j^i - Semipermeability coefficient between layers j and $j+1$ in region i
χ_j^i - Vertical permeability-thickness ratio
κ_j^i - Permeability-thickness product in layer j and region i
ϕ_j - Porosity in layer j
μ_F - Fluid viscosity
μ_{ji} - Viscosity of region i in in layer j
ω_j - Porosity-thickness product in layer j

7. Acknowledgements

We would like to thank Petrobras for the financial support. Finally, this study was financed in part by the Coordenação de Aperfeiçoamento de Pessoal de Nível Superior - Brasil (CAPES) - Finance Code 001, so we would also like to thank CAPES.

References

Barreto, A. B., Peres, A. M., Pires, A. P., et al. (2011). Water injectivity tests on multilayered oil reservoirs. In *Brasil Offshore*. Society of Petroleum Engineers.

Bratvold, R. B., Horne, R. N., et al. (1990). Analysis of pressure-falloff tests following cold-water injection. *SPE Formation Evaluation*, 5(03):293–302.

Buckley, S. E., Leverett, M., et al. (1942). Mechanism of fluid displacement in sands. *Transactions of the AIME*, 146(01):107–116.

CMG (2010). *IMEX User Guide*. Computer Modeling Group.

Cobb, W. M., Ramey Jr, H., Miller, F. G., et al. (1972). Well-test analysis for wells producing commingled zones. *Journal of Petroleum Technology*, 24(01):27–37.

Ehlig-Economides, C. A. and Joseph, J. (1987). A new test for determination of individual layer properties in a multilayered reservoir. *SPE Formation Evaluation*, 2(03):261–283.

Lefkovits, H., Hazebroek, P., Allen, E., Matthews, C., et al. (1961). A study of the behavior of bounded reservoirs composed of stratified layers. *Society of Petroleum Engineers Journal*, 1(01):43–58.

LF Bittencourt Neto, J., Vieira Bela, R., Pesco, S., Barreto, A., et al. (2020a). Laplace domain pressure behavior solution for multilayered composite reservoirs. In *SPE Latin American and Caribbean Petroleum Engineering Conference*. Society of Petroleum Engineers.

LF Bittencourt Neto, J., Vieira Bela, R., Pesco, S., Barreto, A., et al. (2020b). Pressure behavior during injectivity tests-a composite reservoir approach. In *SPE Latin American and Caribbean Petroleum Engineering Conference*. Society of Petroleum Engineers.

Nie, R.-S., Guo, J.-C., Jia, Y.-L., Zhu, S.-Q., Rao, Z., and Zhang, C.-G. (2011). New modelling of transient well test and rate decline analysis for a horizontal well in a multiple-zone reservoir. *Jornal of Geophysiscs and Engineering*, 8:464–476.

Stehfest, H. (1970). Algorithm 368: Numerical inversion of laplace transforms [d5]. *Communications of the ACM*, 13(1):47–49.

Sun, H. and Gao, C. (2017). *Well Test Analysis for Multilayered Reservoirs with Formation Crossflow*. Gulf Professional Publishing.